



HAL
open science

Once in a blue stream. Detection of recent star formation in the NGC 7241 stellar stream with MEGARA

David Martínez-Delgado, Santi Roca-Fàbrega, Armando Gil de Paz, Denis Erkal, Juan Miró-Carretero, Dmitry Makarov, Karina T. Voggel, Ryan Leaman, Walter Boschin, Sarah Pearson, et al.

► To cite this version:

David Martínez-Delgado, Santi Roca-Fàbrega, Armando Gil de Paz, Denis Erkal, Juan Miró-Carretero, et al.. Once in a blue stream. Detection of recent star formation in the NGC 7241 stellar stream with MEGARA. *Astronomy and Astrophysics - A&A*, 2024, 684, 10.1051/0004-6361/202244350 . insu-04567195

HAL Id: insu-04567195

<https://insu.hal.science/insu-04567195>

Submitted on 6 May 2024

HAL is a multi-disciplinary open access archive for the deposit and dissemination of scientific research documents, whether they are published or not. The documents may come from teaching and research institutions in France or abroad, or from public or private research centers.

L'archive ouverte pluridisciplinaire **HAL**, est destinée au dépôt et à la diffusion de documents scientifiques de niveau recherche, publiés ou non, émanant des établissements d'enseignement et de recherche français ou étrangers, des laboratoires publics ou privés.



Distributed under a Creative Commons Attribution 4.0 International License

Once in a blue stream

Detection of recent star formation in the NGC 7241 stellar stream with MEGARA[★]

David Martínez-Delgado^{1,★★}, Santi Roca-Fàbrega^{2,3}, Armando Gil de Paz^{3,4}, Denis Erkal⁵, Juan Miró-Carretero³, Dmitry Makarov⁶, Karina T. Voggel⁷, Ryan Leaman⁸, Walter Bolchin⁹, Sarah Pearson¹⁰, Giuseppe Donatiello¹¹, Evgenii Rubtsov¹², Mohammad Akhlaghi¹³, M. Angeles Gomez-Flechoso^{3,4}, Samane Raji¹⁴, Dustin Lang¹⁵, Adam Block¹⁶, Jesus Gallego^{3,4}, Esperanza Carrasco¹⁷, María Luisa García-Vargas¹⁸, Jorge Iglesias-Páramo¹, Sergio Pascual^{3,4}, Nicolas Cardiel^{3,4}, Ana Pérez-Calpena¹⁸, Africa Castillo-Morales^{3,4}, and Pedro Gómez-Alvarez¹⁸

¹ Instituto de Astrofísica de Andalucía, CSIC, Glorieta de la Astronomía, 18080 Granada, Spain
e-mail: dmartinez@iaa.es

² Lund Observatory, Division of Astrophysics, Department of Physics, Lund University, Box 43, 221 00 Lund, Sweden

³ Departamento de Física de la Tierra y Astrofísica, Universidad Complutense de Madrid, 28040 Madrid, Spain
e-mail: sroca01@ucm.es

⁴ Instituto de Física de Partículas y del Cosmos (IPARCOS), Fac. CC. Físicas, Universidad Complutense de Madrid, Plaza de las Ciencias, 1, 28040 Madrid, Spain

⁵ Department of Physics, University of Surrey, Guildford GU2 7XH, UK

⁶ Special Astrophysical Observatory, Russian Academy of Sciences, Nizhnii Arkhyz 369167, Russia

⁷ Université de Strasbourg, CNRS, Observatoire astronomique de Strasbourg, UMR 7550, 67000 Strasbourg, France

⁸ Department of Astrophysics, University of Vienna, Türkenschanzstraße 17, 1180 Vienna, Austria

⁹ Fundación G. Galilei – INAF (TNG), Rambla J. A. Fernández Pérez 7, 38712 Breña Baja, La Palma, Spain

¹⁰ Center for Cosmology and Particle Physics, Department of Physics, NYU, 726 Broadway, New York, NY 10003, USA

¹¹ UAI – Unione Astrofili Italiani /P.I. Sezione Nazionale di Ricerca Profondo Cielo, 72024 Orta, Italy

¹² Sternberg Astronomical Inst., M.V. Lomonosov Moscow State University, Universitetsky Prospect 13, Moscow 119234, Russia

¹³ Centro de Estudios de Física del Cosmos de Aragón (CEFCA), Unidad Asociada al CSIC, Plaza San Juan 1, 44001 Teruel, Spain

¹⁴ Department of Physics, Yazd University, University Blvd, Safayieh, Yazd, Iran

¹⁵ Perimeter Institute for Theoretical Physics, 31 Caroline St N, Waterloo, Canada

¹⁶ Steward Observatory, Department of Astronomy, University of Arizona, 933 N. Cherry Avenue, Tucson, AZ 85748, USA

¹⁷ Instituto Nacional de Astrofísica, Óptica y Electrónica, Calle Luis Enrique Erro 1, Tonantzintla, Puebla, Mexico

¹⁸ FRACTAL S.L.N.E. Calle Tulipán 2, Portal 13, 1A, 28231 Las Rozas de Madrid, Spain

Received 24 June 2022 / Accepted 13 November 2023

ABSTRACT

Aims. In this work we study the striking case of a narrow blue stream with a possible globular cluster-like progenitor around the NGC 7241 galaxy and its foreground dwarf companion. We want to figure out if the stream was generated by tidal interaction with NGC 7241 or if it first interacted with the foreground dwarf companion and later both fell together toward NGC 7241.

Methods. We used four sets of observations, including a follow-up spectroscopic study of this stream based on data taken with the MEGARA instrument at the 10.4 m Gran Telescopio Canarias using the integral field spectroscopy mode, the Mount Lemmon 0.80 m telescope, the Telescopio Nazionale *Galileo*, the DESI Imaging Legacy surveys, and GALEX archival data. We also used high-resolution zoomed-in cosmological simulations.

Results. Our data suggest that the compact object we detected in the stream is a foreground Milky Way halo star. Near this compact object we detect emission lines overlapping a less compact, bluer, and fainter blob of the stream that is clearly visible in both ultraviolet and optical deep images. From its heliocentric systemic radial velocity derived from the [O III] $\lambda 5007$ Å lines ($V_{\text{sys}} = 1548.58 \pm 1.80$ km s⁻¹) and new UV and optical broadband photometry, we conclude that this overdensity could be the actual core of the stream, with an absolute magnitude of $M_g \sim -10$ and a $g-r = 0.08 \pm 0.11$, consistent with a remnant of a low-mass dwarf satellite undergoing a current episode of star formation. From the width of the stream and assuming a circular orbit, we calculate that the progenitor mass can be typical of a dwarf galaxy, but it could also be substantially lower if the stream is on a very radial orbit or if it was created by tidal interaction with the companion dwarf instead of with NGC 7241. These estimates also suggest that this is one of the lowest mass streams detected to date beyond the Local Group. Finally, we find that blue stellar streams containing star formation regions are commonly predicted by high-resolution cosmological simulations of galaxies lighter than the Milky Way. This scenario is consistent with the processes explaining the bursty star formation history of some dwarf satellites, which are followed by a gas depletion and a fast quenching once they enter within the virial radius of their host galaxies for the first time. Thus, it is likely that the stream's progenitor is undergoing a star formation burst comparable to those that have shaped the star formation history of several Local Group dwarfs in the last few gigayears.

Key words. galaxies: dwarf – galaxies: formation – galaxies: interactions

[★] Reduced spectra are available at the CDS via anonymous ftp to cdsarc.cds.unistra.fr (130.79.128.5) or via <https://cdsarc.cds.unistra.fr/viz-bin/cat/J/A+A/684/A157>

^{★★} Talentia Senior Fellow.

1. Introduction

Star formation in the low- z Universe mostly occurs inside galactic disks through dynamical instabilities (Kennicutt 1998; Leroy et al. 2008). These processes dominate the current star formation rate (SFR) in the Universe, but are not exclusive. Many authors have reported observations of star-forming regions outside galactic disks (e.g., O’Dea et al. 2004; Sengupta et al. 2009; Howk et al. 2018a; Smith et al. 2010). In these regions, a gas shell, a gas stream, or a gas cloud undergoes a strong perturbation, collapses, and generates a new population of stars. Some examples of this process are the star formation clumps observed in boundaries of radio jets and lobes (Graham 1998; Mould et al. 2000; O’Dea et al. 2004), in clouds of extraplanar gas originated by the galactic fountain (Tüllmann et al. 2003; Howk et al. 2018a), or in highly perturbed regions such as the tidal debris left from the first interactions during wet major mergers (Sengupta et al. 2009; Hibbard et al. 2005). If massive enough, this new self-gravitating stellar population leads to the formation of a young star cluster (Howk et al. 2018b) or, in strong tidal interactions, to new objects such as tidal dwarf galaxies (TDGs) (Duc & Mirabel 1998; Duc et al. 2000; Smith et al. 2007, 2010).

Two ingredients are needed in these processes to allow the formation of a new stellar population: the presence of a cold molecular gas cloud and a strong perturbation. Strong perturbations are present in most galactic systems in many forms, from gas sound waves (e.g., SNe shells or AGN jets) to tidal perturbations by companions or non-axisymmetric structures inside galaxies (Buta et al. 2019). In addition to these special conditions, the formation of cold and/or molecular clouds is not seen outside the disk plane. In the disk outskirts, the dynamics of gas is tightly bounded with the circumgalactic medium (CGM) properties. High-mass galaxies develop a warm-hot CGM that inhibits the formation of cold clouds of molecular gas in hydrostatic equilibrium far from the disk region (Kereš et al. 2005). On the other hand, low-mass galactic systems present the prototypical galactic fountain where metal-rich gas is released by SNe winds to the CGM, or even the intergalactic medium (IGM), and quickly cools down and falls back to the disk from large radii. So, there is a strong dependence on the distribution of extraplanar star formation with galaxy virial mass (i.e., CGM virial temperature) (Fraternali 2017). Similarly, it is favored in low-mass systems that cold gas infalling from the IGM through cold flows, or inside gas-rich satellites, penetrates down to the galactic disk and/or condensates inside gas-rich filaments or tidal structures (Fraternali 2017).

The star formation in the tidal tails generated around infalling satellites during gas-rich minor mergers has only been studied in a few works using smoothed-particle hydrodynamic (SPH) simulations (Kapferer et al. 2009). Current studies of extraplanar star formation have mainly focused on the consequences of major mergers and interactions within massive clusters of galaxies (Tüllmann et al. 2003; O’Dea et al. 2004; Leroy et al. 2008; Werk et al. 2008; McDonald et al. 2012). Furthermore, predictions from the theory of galaxy formation and evolution points toward a relation between the minimum radius reached by gas inside infalling satellites before being ram-pressure stripped and the properties of the gas surrounding the central galaxy (Hester 2006), which are tightly linked with the total mass of the central galaxy (Birboim & Dekel 2003). If the central galaxy is a low-mass system (i.e., if it has not developed a dense warm-hot CGM), the satellite can reach lower

radii before it is totally ram-pressure stripped. In this situation the satellite’s gas can shock with the central galaxy HI (from the galactic fountain or inside the disk) and produce extraplanar star formation (Noreña et al. 2019). In this situation, newborn stars follow an orbit similar to that of the infalling galaxy (Lim et al. 2018) and, as a result, we would observe a blue stellar stream.

NGC 7241 is a galaxy that is transitioning from a low-mass scenario, with no warm-hot corona, to a high-mass scenario (like the MW), with a spatially extended HI gas disk (Leaman et al. 2015). The first inspections of this galactic system in the UV images from GALEX seemed to show that this edge-on disk galaxy has a strong off-plane star formation, although this galaxy shows no morphological evidence of a recent interaction triggering it. The lack of morphological perturbations was also in contradiction with the HI observations by Giovanelli & Haynes (1984) that showed evidence of the presence of a possible dwarf companion in the field. More recently, Leaman et al. (2015) confirmed the presence of this companion, an actively star-forming dwarf in the foreground of the NGC 7241 galactic disk. The foreground dwarf hosts the strong off-plane star formation observed in the GALEX images. Leaman et al. (2015) also discovered a nearby stellar tidal stream; using $H\alpha$, they studied the kinematics of all the components in the system and concluded that the stream is associated with the star-forming companion. However, the analysis of the connection between the possible companion and NGC 7241 was not conclusive. The authors also studied the companion’s SFR and observed that it is one order of magnitude higher than expected for a normal galaxy of its mass. These results, in addition to the absence of strong morphology perturbations and of an enhanced SF in the NGC 7241 disk, pointed toward an unknown but potentially complex interaction history. In particular, it is under study to determine whether the infall of a small galactic system toward the companion could create the observed narrow tidal stream.

In this paper we present follow-up spectroscopic observation of the blue stream of NGC 7241, with the aim of constraining the nature of a compact object found inside the stream. In addition to undertaking a new photometry and structural study of this stream, we explore the formation scenario of this rare blue stream in the nearby Universe using cosmological simulations. In this context, we explore whether our observations of a possible star-forming progenitor are showing a process similar to the one that shaped the star formation history (SFH) of some dwarfs in the Local Group, which show an early star formation peak followed by fast quenching (Weisz et al. 2015).

2. Observations and data reduction

2.1. Gran Telescopio Canarias MEGARA spectroscopy observations

The brightest region of the NGC 7241 stream was observed with the Multi Espectrógrafo en GTC de Alta Resolución para Astronomía (MEGARA) instrument at the Gran Telescopio Canarias (GTC) on the night of June 6, 2020, using the Integral Field Unit (IFU) in the LR-B spectral configuration with a power resolution of $R \sim 5000$ in the wavelength interval 4332–5199 Å, for a total exposure time of 3600 s. The target field, with a field of view of $12.5'' \times 11.3''$ (purple filled square in Fig. 1, upper right panel), was centered on the position of the blue compact source embedded in the stream (hereafter GC-CAND). This observing

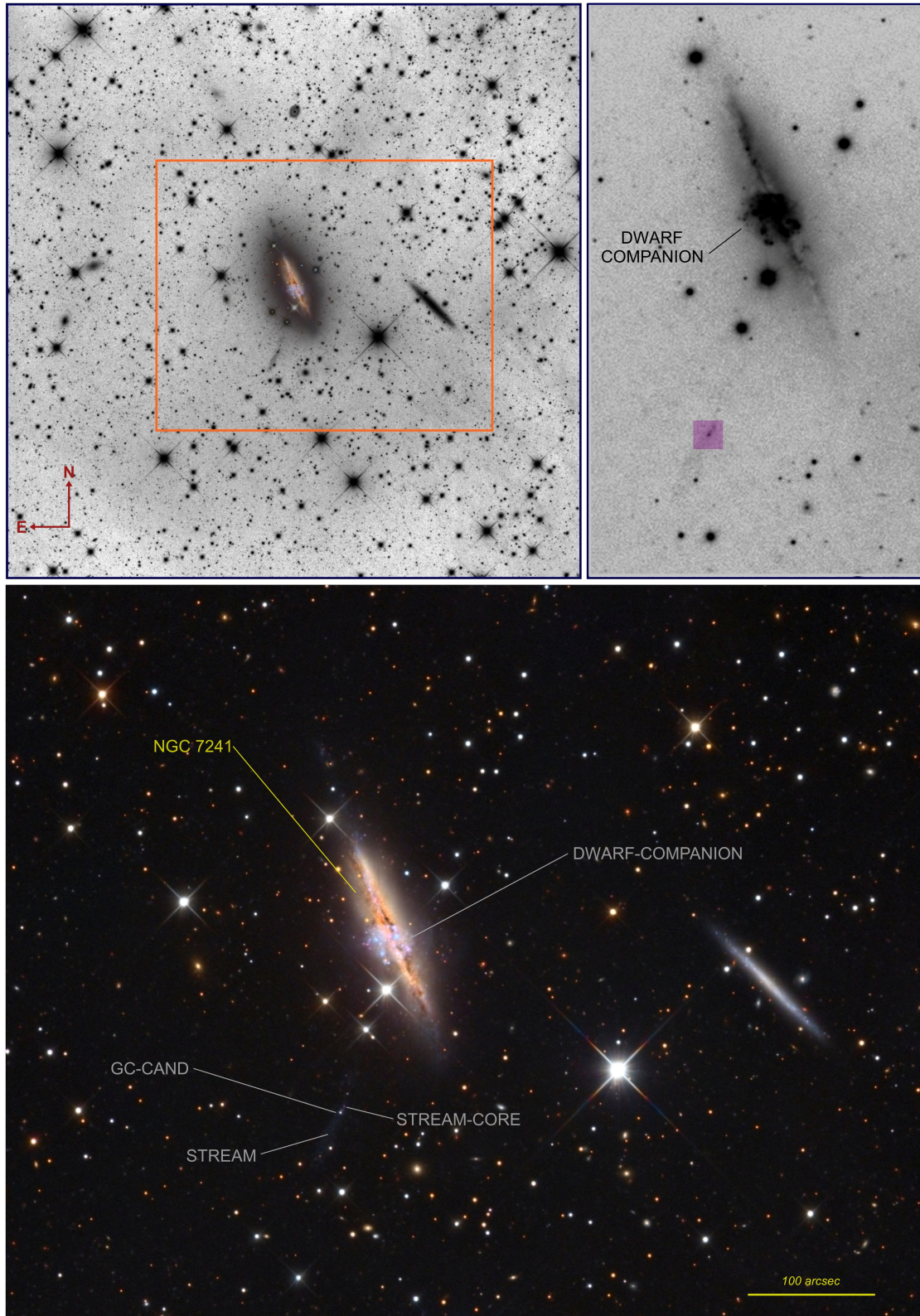


Fig. 1. NGC 7241 images including the blue stream and the dwarf companion projected on its center. *Upper left:* L -filter wide-field image obtained with the Mount Lemmon 0.80 m $f/7$ Ritchey-Chrétien telescope. The total field of view is 22.5×22.5 arcmin. The red square is the field of the full color image displayed in the bottom panel. *Upper right:* u' -band observations obtained with DOLoRes at the TNG 3.58 m at the La Palma observatory. The purple filled square is the field of view of the MEGARA IFU field which is placed on the compact object in the stream. *Bottom panel:* magnified full-color version of the deep image obtained with the Mount Lemmon 0.80 m telescope, including the NGC 7241 central region (red square in upper left panel).

time was split into three consecutive exposures of 1200 s to allow for cosmic-ray removal. The three individual exposures were processed using the MEGARA Data Reduction Pipeline version 0.10.1 (MEGARADRP; see Pascual et al. 2018) and combined to generate the final row-stacked spectra (RSS) FITS frame that was used for our analysis.

The data processing included bias subtraction, gain normalization of the two amplifiers, tracing and extraction of the 567 objects plus the 56 sky fiber spectra, wavelength calibration, flat-fielding correction of the blue-to-red and fiber-to-fiber response, and absolute flux calibration. The fiber tracing, extraction modeling, and flat-fielding (TRACEMAP, MODELMAP, and FIBERFLAT recipes, respectively) were performed using halogen lamp observations taken at the end of night. The wavelength calibration was performed using observations of the five ThAr lamps available at the Instrument Calibration Module (ICM). The standard deviation of our wavelength calibration solution achieved was 0.021 \AA for a reciprocal linear dispersion of $0.22 \text{ \AA pix}^{-1}$. In order to perform the absolute calibration of these data the spectrophotometric standard star HR 5501 was also observed during that night and processed using the MEGARADRP. More information on the processing of MEGARA data using the MEGARADRP can be found in García-Vargas et al. (2020).

2.2. Mount Lemmon 0.80-m imaging observations

We collected deep imaging of the field around NGC 7241 at the Mount Lemmon Sky Center (Steward Observatory, University of Arizona) with an 80 cm aperture $f/7$ Ritchey-Chrétien telescope. We used a SBIG STX16803 CCD camera that provided a pixel scale of $0.33'' \text{ pixels}^{-1}$ over a $22.5' \times 22.5'$ field of view. We obtained a set of 32 individual 1200-second images with an Astrodon Gen2 Tru-Balance E-series luminance filter over several photometric nights between 2017 June and 2017 July. We obtained this data by remote observations. In the upper left panel of Fig. 1 we show the image we took using the luminance filter, a wide-band nearly top-hat filter that transmits from $400 \lesssim \lambda \text{ (nm)} \lesssim 700$, and broadly covers the more familiar g and r bands. Each individual exposure was reduced following standard image processing procedures for dark subtraction, bias correction, and flat-fielding adopted for the larger stream survey (Martínez-Delgado et al. 2010). The images were combined to create a final co-added image with a total exposure time of 38 400 s.

2.3. Telescopio Nazionale Galileo imaging observations

We took deep images of the field of NGC 7241 with the Device Optimized for the Low Resolution (DOLoRes) instrument at the 3.58 m Italian Telescopio Nazionale Galileo (TNG, Roque de Los Muchachos Observatory, La Palma, Spain) on December 10, 2018. These observations include 9×300 s exposures in the u' band (binning 2×2 , pixel scale $0.504''$) with a field of view of $8.6' \times 8.6'$ and a seeing measured in this band of $\sim 1.3''$ (see Fig. 1, upper right panel). A zoom-in region of the stream region from this u' -band image is also showed in Fig. 2 (upper panel).

The pre-processing of the data was performed in a standard way using IRAF tasks (i.e., dividing the trimmed and bias subtracted frames by a master flat field produced from multiple twilight sky-flat exposures). Then a final image was obtained by performing a median stack of the pre-processed images. In the last stage the astrometric calibration of this image was performed using the astrometry.net tool (Lang et al. 2010).

2.4. DESI Imaging Legacy surveys and GALEX archival data

The DESI Legacy Imaging Surveys compile optical data in three optical bands (g , r , and z) obtained by three different imaging projects: The DECam Legacy Survey (DECaLS), the Beijing-Arizona Sky Survey (BASS), and the Mayall z -band Legacy Survey (MzLS) (Zou et al. 2019; Dey et al. 2019). The DESI Legacy Imaging Survey data releases also include re-reduced public DECam data from the DES (Abbott et al. 2018). An image cutout centered on NGC 7241 were subsequently obtained by coadding images of these systems taken by the DES (Dark Energy Survey Collaboration 2016) using the DECam. These data were reprocessed using the LEGACYPIPE software of the DESI Legacy Imaging Surveys (see, e.g., Fig. 2 in Martínez-Delgado et al. 2023). In short, each image including our target galaxy is astrometrically calibrated to *Gaia*-DR2 and photometrically calibrated to the Pan-STARRS PS1 survey, and subsequently resampled to a common pixel grid and summed with inverse-variance weighting. Figure 3 (upper panel) shows the resulting coadded image cutout of the NGC 7241 stream galaxy, which was used to derive the photometry of stream in the g , r , and z bands (see Sect. 3.2).

The region around NGC 7241 was also observed by the Galaxy Evolution Explorer (GALEX; Martin et al. 2005) on August 23, 2003, simultaneously in its far-ultraviolet (FUV) and near-ultraviolet (NUV) bands as part of the GALEX All-sky Imaging Survey (AIS). The valid exposure times acquired on this field were 120 s in the FUV channel and 175 s in the NUV channel.

3. Results

3.1. Radial velocity from MEGARA observations

The blue stream of NGC 7241 (see Fig. 1, bottom panel) is a tail $\sim 45''$ in length that seems to emanate from a bright compact object (GC-CAND) located at a position angle of ~ 150 deg (measured from north to east). The visual inspection of the RSS 2D FITS file created by the MEGARADRP¹ from the observation centered at the GC-CAND (see Sect. 2.1) reveals the presence of two faint emission lines in several spaxels that correspond to $H\beta$ and $[\text{O III}]\lambda 5007 \text{ \AA}$ at the approximate redshift of NGC 7241 ($z \sim 0.0048$ or $1447 \pm 1 \text{ km s}^{-1}$; Lu et al. 1993). Since the location of these lines does not coincide with the brightest spaxels in the continuum, we decided to determine the heliocentric radial velocity map in the vicinity of the possible nucleus of the NGC 7241 stream using these data. For this purpose we made use of the analysis and visualization tools distributed along with the MEGARADRP, namely the `analyzerss` and `visualization` codes (see Castillo-Morales & Gil de Paz 2020). The first code was used to measure the intensity and recession velocity of every emission line detected in any spaxel with a line peak signal-to-noise ratio (S/N) above a given threshold along with the corresponding errors². Interestingly, in our case we found a coherent structure with emission above $S/N = 5$ in 11(5) spaxels in the $H\beta$ ($[\text{O III}]\lambda 5007 \text{ \AA}$) line, but not at the position of the GC-CAND. This emission emanates from a second, fainter overdensity just north of the GC-CAND, which is visible in the

¹ More information on the processing of the MEGARA data using the MEGARADRP can be found in García-Vargas et al. (2020).

² The errors in radial velocity were obtained from the covariance matrix as part of the analysis performed by the LMFIT Python package included in MEGARATOOLS within the MEGARADRP using a Levenberg-Marquardt least-squares minimization method.

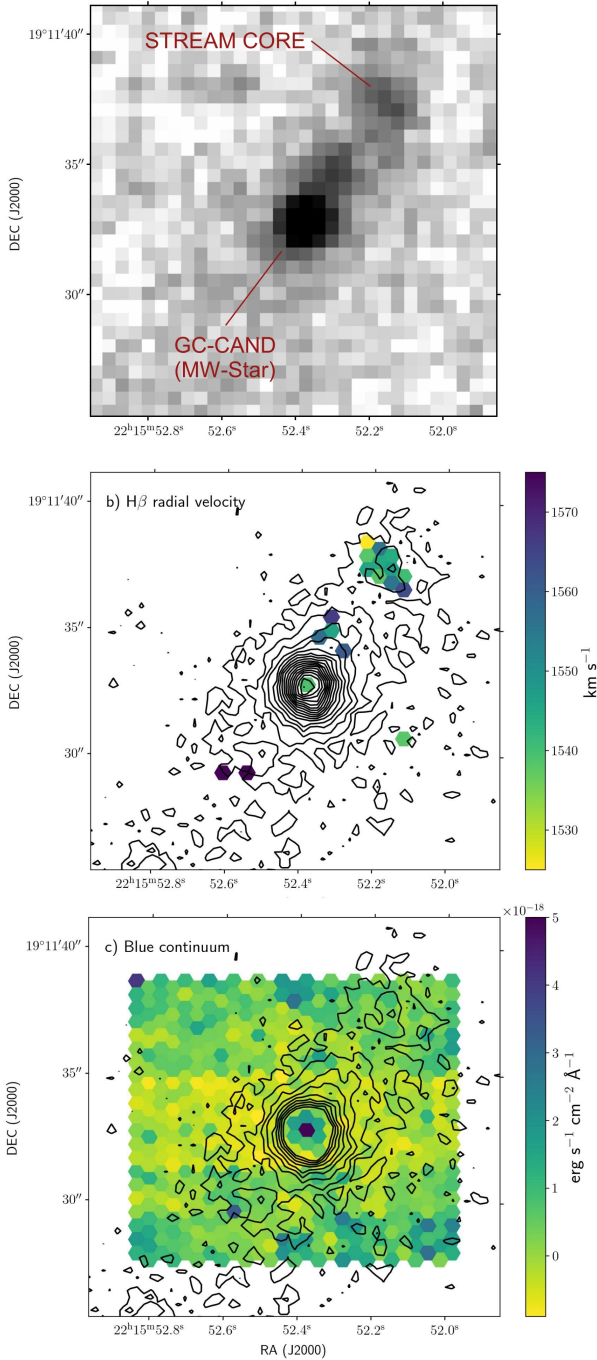


Fig. 2. TNG u' -band image and MEGARA spectroscopy of the blue stellar stream in the NGC 7241 halo. *Top*: zoom-in on the region in the position of the stream taken from the TNG u' -band image. It is centered in the compact object targeted in our campaign as the possible progenitor of the stream. The image also shows a second fainter overdensity at ~ 5 arcsec northwest (top right) labeled as the stream core. *Middle*: heliocentric radial velocity obtained from the emission in $H\beta$ line detected in the MEGARA LR-B data. Two emission sources are observed, a compact one in the center and the second in the top right corner. The g -band DESI Imaging Legacy data contours are overplotted. The g -band contours shown correspond to the range between 28 and 31 AB mag arcsec $^{-2}$ and are equally spaced in linear (flux) scale. *Bottom*: continuum image of the stream nucleus candidate obtained after averaging the flux from the MEGARA LR-B datacube in the (rest-frame) wavelength range between 480–484 nm and 487–495 nm. The same g -band contours as those used for panel b, except for those brighter than 28.7 AB mag, are plotted here.

u' -band TNG image (indicated in Fig. 2, upper panel) and in the DES images (red circle in Fig. 3, bottom panel). Following discussion on the actual progenitor of the NGC 7241 stream (see Sect. 4.2), we named this feature STREAM-CORE. From the spectrum of these 11 spaxels we obtained an observed (topocentric) wavelength for the bluest of the two lines detected of $4885.987 \pm 0.027 \text{ \AA}$, which corresponds to a heliocentric radial velocity for the STREAM-CORE of $1547.92 \pm 1.65 \text{ km s}^{-1}$ if we assume that this line is $H\beta$, given that the topocentric to heliocentric correction is $+24.25 \text{ km s}^{-1}$. Adding up the flux from all these spaxels, the best-fitting observed wavelength for the reddest line detected is $5032.301 \pm 0.030 \text{ \AA}$ or a heliocentric radial velocity of $1547.59 \pm 1.80 \text{ km s}^{-1}$, assuming this corresponds to $[O III]\lambda 5007 \text{ \AA}$. The results of the best fits to both lines are shown in Fig. 4. We note that the standard deviation of our wavelength calibration solution is 1.1 km s^{-1} , while the reciprocal dispersion yields $\sim 12 \text{ km s}^{-1}$ at these wavelengths.

The only absorption or emission detail visible in the spectrum obtained at the GC-CAND location is at 4857.0 \AA , with a significance of about $5\text{--}6\sigma$ (see Fig. 4, bottom panel). Assuming the absorption is $H\beta$ we see that it is blueshifted by -269 km s^{-1} . To determine the radial velocity from this line we needed to increase the S/N, which was originally ~ 2 . To do this we reduced the resolution from $R \sim 5000$ to $R \sim 2500$ using Gaussian smoothing and rebinned the spectrum to the scale of 2 pix per full width at half maximum (FWHM). With these operations we achieved a $S/N \sim 9$. Finally, we fitted the resulting spectrum by the PEGASE.HR stellar population models (Le Borgne et al. 2004) using the NBURSTS software (Chilingarian et al. 2007). The resulting radial velocity for the GC-CAND is $V_h = -233 \pm 33 \text{ km s}^{-1}$ with respect to the Solar System barycenter³.

3.2. Photometry and structural properties

The photometry of the NGC 7241 stream in the DES images was carried out using GNU Astronomy Utilities (Gnuastro)⁴. All the measurements were done using Gnuastro's MAKECATALOG on the sky-subtracted image generated by Gnuastro's NOISECHISEL (Akhlaghi & Ichikawa 2015; Akhlaghi 2019). This tool was developed with emphasis on the detection of low surface brightness, diffuse sources. The surface brightness limits of the images, giving the depth of the image, were calculated following the standard method of Román et al. (2020): the 3σ measured value on a 100 arcsec^2 aperture and yield $28.99 \text{ [mag arcsec}^{-2}]$ for g , $28.42 \text{ [mag arcsec}^{-2}]$ for r , and $28.28 \text{ [mag arcsec}^{-2}]$ for u .

We used NOISECHISEL (Gnuastro) to perform sky-subtraction on the DESI images previously processed with the LEGACYPIPE (see Sect. 2.4). For this purpose the image is tessellated; the tiles have a configurable number of pixels (typically 40×40). The sky background in the tiles with detection is obtained by interpolation of the signal in the neighboring tiles with no detection, and then subtracted locally. In this way the

³ We find that the feature resembling a P Cygni absorption component is due to a sky subtraction residual that can be seen in the original high-resolution spectrum of STREAM-CORE near $H\beta$ at around 4878 \AA . This feature does not affect the determination of the radial velocity, line flux, or line ratios in STREAM-CORE given that it is well separated from our line of interest. Not only is this feature out of the line window, but it was also excluded from the continuum windows used to measure the continuum level and the continuum rms (needed to compute the errors in the line flux).

⁴ <http://www.gnu.org/software/gnuastro>

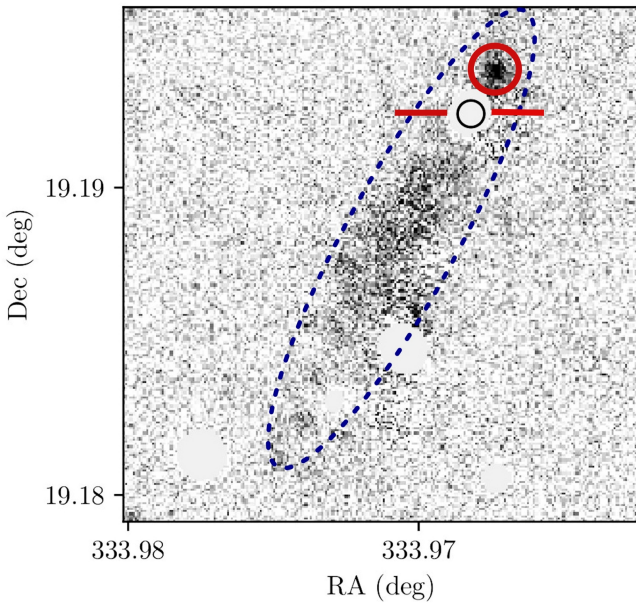
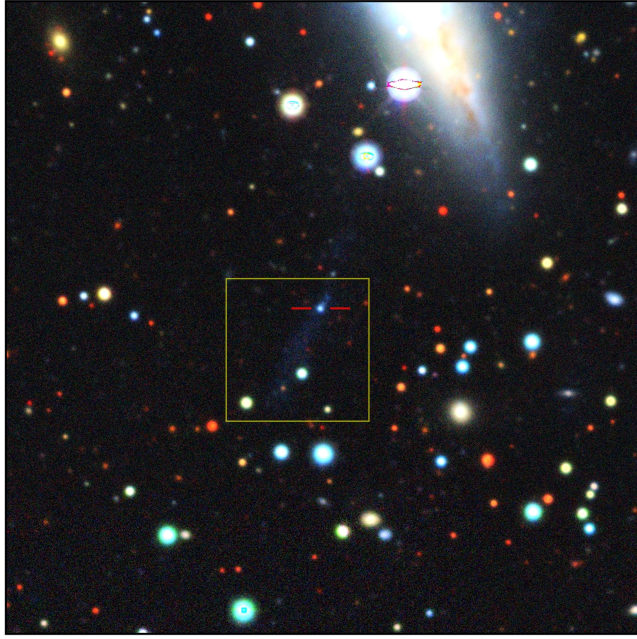


Fig. 3. Photometry analysis of the NGC 7241 blue stream. *Upper panel:* image cutout obtained from the DESI Legacy surveys data with LEGACYPIPE centered in the compact object GC-CAND (indicated by two red lines) embedded in the NGC 7241 stream and classified as a foreground halo star in our study (see Sect. 4.2). The total field of view of this image is 5×5 arcmin. The orange square indicates the extent of the figure shown in the bottom panel. *Bottom panel:* apertures used to perform the photometry of the stream (dashed blue line) and its possible progenitor STREAM-CORE (red circle) are overlapped in a r -band DESI LS image of the stream. The source GC-CAND (black circle between the two red lines) was also masked to derive the results given in Table 2.

environment of the stream is taken into consideration for the calculation of the sky background. The photometry is then measured on the image once the sky background has been subtracted. The magnitude and the surface brightness (SB) are measured for the r and g bands together with their color ($g - r$) for the stream

and STREAM-CORE (red circle in Fig. 3, bottom panel). The results are given in Table 1. The measurement for the stream was carried out on an elliptical aperture encompassing most of the stream (dashed line in Fig. 3, bottom panel). We masked the foreground stars and background objects, which includes the star rejected as nucleus of the stream (GC-CAND). Measurements were carried out with and without masking the compact structure (corresponding to the rows stream and stream+core, respectively, in Table 1). This table also shows the measurements of the possible progenitor of the stream itself (labeled STREAM-CORE), showing that it is bluer than the stream itself. In order to verify that the ellipse was a good enough fit to the stream contour, and that the measurements were thus correct, the surface brightness was also measured on circular apertures placed carefully on the stream to ensure they were completely overlapping with it. The results were within 0.04 and 0.11 [mag arcsec $^{-2}$] of the measurements on the elliptical aperture for g and r , respectively, which shows that our results do not depend on the exact chosen aperture.

The photometry of the stream was also obtained in the u' band using the TNG data of NGC 7241 (described in Sect. 2.2) and the same elliptical aperture and masking as for the bands g and r . To find the zeropoint of the u' -band image (30.18 ± 0.04 mag), matched aperture photometry was used in comparison with Sloan Digital Sky Survey (SDSS) images. To this end, we ran NOISECHISEL and Segment and selected the clumps with $S/N > 10$ and axis-ratio > 0.85 in the u' -band image. An aperture of radius 2 arcsec was then placed over them in the TNG and SDSS images (using MAKEPROFILES) and the photometry over the apertures obtained with MAKECATALOG. The zeropoint was estimated by calculating the difference (for stars with magnitude between 17 and 20).

The u' -band photometry is also included in Table 1 and discussed in Sect. 4.3. Finally, the width of the stellar stream was estimated for three points along the stream (maximum, minimum, and intermediate width) assuming a distance of 22.5 kpc. The results are given in Table 2.

Despite the low exposure times of the GALEX images, the emission from the stellar stream is also detected in the two bands, due certainly to its very blue color. Using circular apertures of 15 arcsec (approximately three times the FWHM of the GALEX PSF) in radius centered on RA(J2000) = 22:15:52.38 and Dec(J2000) = 19:11:29.3, we estimated the FUV and NUV aperture magnitudes of 20.10 mag and 20.06 mag with estimated errors between 0.05–0.11 mag and 0.16–0.22 mag, respectively. The $FUV - NUV$ color inferred is $(FUV - NUV) = 0.045$ with an error no lower than 0.18 mag. The UV photometry was performed as in Gil de Paz et al. (2007), and takes into account the highly Poissonian regime of the GALEX AIS images and the potential presence of low-frequency background variations. The blue color found corresponds to a roughly flat f_ν spectrum, and is comparable to that measured in star-forming dwarfs and the outermost regions of spiral disks (see Bouquin et al. 2018), including extended ultraviolet (XUV) disks, and it is commonly associated with regions of active recent star formation and low dust content.

3.3. Metallicity

We estimate the metal abundance of the ISM in the stream of NGC 7241 using the two emission lines clearly detected in our optical spectra, namely [O III] $\lambda 5007$ Å and H β . The best-fitting Gaussians to each of these two lines after adding the spectra of the 11 spaxels where line emission is clearly detected ($S/N \gtrsim 5$

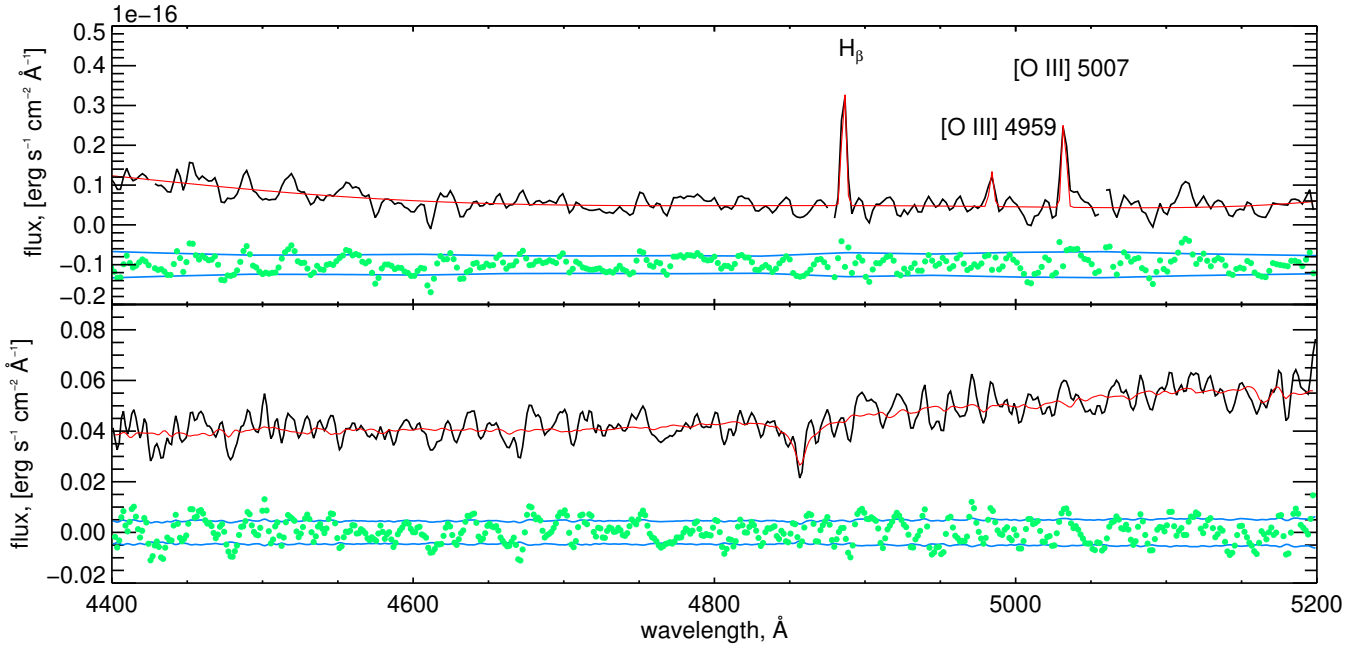


Fig. 4. MEGARA spectroscopy of the NGC 7241 blue stream. *Top panel:* MEGARA LR-B spectrum of the northwest region showing line emission (see top right region of panel b in Fig. 2) fitted by a multi-Gaussian for emission lines with an additive polynomial for continuum. The $H\beta$ line and the $[O\text{ III}]\lambda\lambda 4959, 5007\text{ \AA}$ doublet are identified along with their positions for a redshift $z = 0.00515$. *Bottom panel:* spectrum of the compact source embedded in the stream fitted by the PEGASE.HR stellar population models using the NBURSTS program. The black line represents the smoothed spectrum of the object and the red line corresponds to the fit. The blue lines and green dots show the flux errors and the data residuals (shifted to -0.1 for the top panel).

at the peak of the line) yield a $[O\text{ III}]\lambda 5007/H\beta$ line ratio of $-0.23^{+0.14}_{-0.21}$. Alternatively, the direct sums of the fluxes above the continuum in the (rest-frame) range between 4855 \AA and 4867 \AA yield a ratio of $-0.09^{+0.16}_{-0.27}$. Based exclusively on this single-line ratio, we cannot obtain too much information about the ionization properties in the possible progenitor of the stream STREAM-CORE (on the conditions of the gas nor the ionizing spectrum). This line ratio, according to the typical values measured in HII regions in the normal galaxies included in the CALIFA sample (see top left panel in Fig. 7 in Morisset et al. 2016), favors an oxygen abundance most likely in the range $8.35 < 12 + \log(O/H) < 8.55$ (see their colorbar), or between $0.4 \times Z_{\odot}$ and $0.63 \times Z_{\odot}$ (adopting a solar oxygen abundance value of $\log A(O) = 8.75$; Bergemann et al. 2021).

4. Discussion

4.1. The NGC 7241 and its dwarf companion

In agreement with the footprints of an NGC 7241 companion in the HI distribution (Giovanelli & Haynes 1984) and the final confirmation by Leaman et al. (2015), we show that the dwarf irregular that overlaps the main body of NGC 7241 is clearly visible in the Mount Lemmon 0.80-m deep image (Fig. 1, bottom panel). Hereafter we refer to this new system as the DWARF-COMPANION.

For the superimposed DWARF-COMPANION object (see Fig. 1, top right panel) in Leaman et al. (2015) the authors estimate a $M_{*} \sim 1.5 \times 10^8 M_{\odot}$, also obtained from SED fitting. Though very uncertain, the size and $H\alpha$ velocity dispersion of the DWARF-COMPANION imply a dynamical mass of order $\sim 10^8 M_{\odot}$, so this would be a baryon dominated object.

Using this data on the total mass of each galactic system, in the following sections we focus on the origin and properties of the blue stream detected in the NGC 7241 and its dwarf companion's neighborhood.

4.2. Determining the progenitor of the blue stellar stream

As mentioned in Sect. 3.1, the blue stream around NGC 7241 seems to emanate from a bright compact object that we named GC-CAND, which is close to another bright but fainter structure that we call STREAM-CORE. In this section we study which of these two objects is the best candidate to be the stream's progenitor.

GC-CAND (RA = 22:15:52.4 Dec = +19:11:32.9) is an object that was also cataloged in the *Gaia* early DR3 (Gaia Collaboration 2021). It has a *Gaia* G magnitude of $G = 20.2$ with the assumed distance this comes out to absolute G magnitude of $M_G = -11.5$, which roughly corresponds to $M_V = -11$. This absolute magnitude places this source at the very bright end of globular clusters (GCs; $M_V < -10$), where we know that more than 50% of the sources are the relic nuclear star cluster of the galaxy that is being stripped (Voggel et al. 2019). Streams with such embedded former nuclei have been discovered in other galaxies (e.g., Jennings et al. 2015). GC-CAND also has a larger *Gaia* $BP - RP$ excess factor similar to what is seen for GCs and nuclei in nearby galaxies (Voggel et al. 2020). *Gaia* proper motions have large errors at these faint magnitudes and its proper motion in the RA direction is detected at the 2.5σ level, which is not significant enough to clearly consider it a foreground star. Therefore, in order to confirm whether the GC-CAND compact object is associated with the stream, a radial velocity measurement is required. In Sect. 3.1 we show that we obtain a velocity of $V_{h_i} = -233 \pm 33\text{ km s}^{-1}$ with

Table 1. Photometry results for the NGC 7241 stream from Gnuastro, including the data from the stream, the structure labeled STREAM-CORE, and the combined data (TOTAL).

Source	Area (pixels)	Area (as ²)	m_g	m_r (mag)	m_u	$\langle\mu_g\rangle$	$\langle\mu_r\rangle$ (mag as ⁻²)	$\langle\mu_u\rangle$	$\langle g-r\rangle_{\text{stream}}$ (mag)
STREAM	7037	483.05	19.23 ± 0.01	19.07 ± 0.02	18.11 ± 0.005	25.94	25.78	24.82	0.16 ± 0.03
CORE	166	11.39	22.21 ± 0.05	22.13 ± 0.06	22.22 ± 0.03	24.85	24.77	24.23	0.08 ± 0.11
TOTAL	7203	494.44	19.16 ± 0.01	19.01 ± 0.02	18.07 ± 0.005	25.90	25.74	24.80	0.15 ± 0.03

respect to the Solar System barycenter; therefore, this compact object is not associated with NGC 7241, which has a systemic velocity of about 1500 km s^{-1} , but is an accidental foreground Milky Way star. To explore this further, we make a simple estimate of the velocity range expected in this line of sight using the SDSS DR16 spectra archive (Ahumada et al. 2020). Within a 30 arcmin cone around the object, there are ~ 50 stars with observed SDSS spectra. Their heliocentric velocities range from -560 to $+125$ with a median value of -54 and a standard deviation of 89 km s^{-1} , estimated by the median absolute deviation. The star velocity distribution shows the second peak near -200 km s^{-1} and that 8 out of 50 stars have a velocity lower than -230 km s^{-1} . Thus, we conclude that GC-CAND has a radial velocity that is typical for Galactic halo stars, and that it cannot be the core of this stellar stream.

The second bright source we detected close to the stream's geometrical center is the STREAM-CORE. From our broadband photometry (see Table 1) we obtained that it would have an absolute magnitude of $M_g \sim -10$ at the distance of NGC 7241. We also find that its color is bluer than that of the stream, as expected from the emission observed only in this region in the MEGARA spectra (see discussion in Sect. 3.1 and Fig. 2, center panel). In Sect. 3.1 we showed that the systemic radial velocity of the STREAM-CORE region is $1547.92 \pm 1.65 \text{ km s}^{-1}$ (from H β in emission), this value is similar to that of both NGC 7241 and its DWARF-COMPANION, so it is not a strong statement to assume that the STREAM-CORE is somehow related with these systems. In addition, the shape of the stream around the position of the STREAM-CORE (see Fig. 3, upper panel) resembles the typical structure of a tidally stripped dwarf galaxy (see, e.g., Wang et al. 2022). Its location in the geometrical center of the stream, radial velocity, color, and shape allow us to conclude that this overdensity is likely the actual progenitor of the stream, and that it is currently undergoing an episode of induced star formation by the tidal interaction with the NGC 7241 or its foreground dwarf companion. The presence of gas in the progenitor of the stream is essential for the formation of new stars, and this suggests that STREAM-CORE cannot be a typical globular cluster (since they have no gas), but that it is probably the main body of an accreted dwarf satellite.

4.3. Properties of the blue stream's progenitor

In order to better understand the NGC 7241 stream, we can make a quantitative estimate of what should have been the NGC 7241 stream progenitor's mass using the results of Johnston et al. (2001) and Erkal et al. (2016), who derived mass estimates for stream progenitors assuming that the stream plane is viewed face-on or edge-on, respectively. These estimates work by determining how the orbits of stars in a given potential fan out once they are ejected from the progenitor and connecting this to the progenitor's dynamical mass.

Table 2. Minimum, maximum, and median estimations of the NGC 7241 stellar stream on-sky width measurements, including n estimation of its physical width assuming a distance to the stream of 22.4 Mpc (Leaman et al. 2015).

	RA (deg)	Dec (deg)	Width (arcsec)	Width (kpc)
Max.	333.97123	19.18.6971	11.960	0.80
Min.	333.96934	19.190611	7.372	1.30
Med.	333.97307	19.183051	8.798	0.95

First, we make the computations assuming that the stream is associated with the central galaxy, not with the dwarf and is seen face-on. Assuming that the stream is on a circular orbit at 20 kpc and that the circular velocity at this radius using the mass estimations in Sect. 4.1, is 202 km s^{-1} , we can use Eq. (12) in Johnston et al. (2001) to obtain that the progenitor mass of the stream is between 1.3 and $5.5 \times 10^7 M_\odot$ using respectively the minimum and maximum width of the stream (see Table 2). We note that this mass estimate is linearly proportional to the stream's pericenter, and thus the progenitor mass could be substantially lower if the stream is on an eccentric orbit at apocenter at the present day. Alternatively, if we assume that we are observing the stream edge-on, we can use the results of Erkal et al. (2016, Eq. (23)), and we obtain a progenitor mass of $6.2 \times 10^7 - 2.7 \times 10^8 M_\odot$ respectively for the minimum and maximum stream width (Table 2). We note that these mass estimates are much lower than for a stream with the same width in the Milky Way since NGC 7241 is a much less massive galaxy, which yields a larger tidal radius (i.e., width) for the stream presented in this work.

Similarly, we can obtain the progenitor's mass assuming that the stream is linked to the DWARF-COMPANION and not to the central galaxy. Using the Johnston et al. (2001) approach (its Eq. (12)) and the DWARF-COMPANION mass estimations obtained in Sect. 4.1 we find that the progenitor mass of the stream should be as low as $3.2 \times 10^4 - 1.4 \times 10^5 M_\odot$.

We note that these estimates suggest that if the stream is on a near circular orbit around NGC 7241, its progenitor is likely a dwarf galaxy stream. Otherwise, if it is on a very radial orbit pointing toward NGC 7241 or if it is orbiting the DWARF-COMPANION, then it could come from a lower mass system like a globular cluster.

Interestingly, the stream width increases with projected distance from NGC 7241/DWARF-COMPANION (see, e.g., Fig. 1). If the stream is on a very eccentric orbit, this may be due to the characteristic shell-like debris, which causes the stream width to increase with radius (see, e.g., Fig. 8 in Hendel & Johnston 2015). Alternatively, if there is a strong distance gradient along the stream, where the parts of the

stream that are closest to the center of NGC 7241/DWARF-COMPANION in projection are in fact the farthest away from us in 3D, it is possible that the most distant debris is too diffuse to observe. The change in the apparent width of the stream could, in that case, merely be an observational effect. If the stream plane is instead being viewed close to edge-on, the change in the stream width could be due to an overlap with different parts of the stream along the line of sight. The specific viewing angle can have a large impact on how we interpret tidal debris (e.g., Barnes & Hibbard 2009), and can lead to apparent asymmetric observations of intrinsically symmetric tidal features. Finally, the stream could physically be asymmetric in nature. Recent data from the Milky Way have revealed that several stellar streams are asymmetric (e.g., Jhelum: Bonaca et al. 2019 and Pal 5: Bernard et al. 2016; Bonaca et al. 2020). Asymmetric stellar streams can be produced through various mechanisms such as interactions with galactic bars (Price-Whelan et al. 2016b; Erkal et al. 2017; Pearson et al. 2017), heating of parts of the streams due to interactions with dark substructure (e.g., Johnston et al. 2002; Ibata et al. 2002; Bonaca et al. 2014), interactions with nearby systems, or specific orbit families within the parent potential causing parts of the stream to “fan out” (e.g., Pearson et al. 2015; Fardal et al. 2015; Price-Whelan et al. 2016a; Yavetz et al. 2021). It is unclear from the edge-on view of NGC 7241 whether the galaxy hosts a bar, as we do not observe any evidence of an x-shaped central structure typically found in barred spirals (e.g., Bureau et al. 2006), but it is clear that the stream could be perturbed by the presence of the second object in the system, NGC 7241 or DWARF-COMPANION. Additionally, if interaction with the bar was the cause, the stream would have already needed to have a close pass with the center of NGC 7241, but no evidence of such an interaction is present in the system. Deeper data in the future will hopefully allow us to distinguish between the possible scenarios discussed in this section.

4.4. NGC 7241: Possible host galaxy of the blue stellar stream

With the mass estimations presented in Sect. 4.1 in hand, if the stellar stream had been generated by the tidal interaction with NGC 7241 and if it had a mass of $M_{\text{stream}} \sim 2 \times 10^7 M_{\odot}$ (Sect. 4.3), then its tidal radius would be $R_{\text{tid}} \sim 823$ pc or $\sim 8''$. Conversely, the tidal radius for the object with respect to the potential of the baryon dominated DWARF-COMPANION with a mass $M_{\text{stream}} \sim 1 \times 10^5 M_{\odot}$ would be $R_{\text{tid}} \sim 600$ pc or $\sim 6''$.

In the previous sections we showed that the width of the stream ranges from 800 pc to 1.3 kpc. These values are larger than the tidal radii crudely estimated from the mass profile and projected distance of NGC 7241, and also than the value derived from the companion dwarfs’ mass, so it would seem sensible to assume that the disrupting system could be dominated either by the tidal influences from the potential of NGC 7241 or by those from the dwarf galaxy companion alone. This result is highly sensitive to the original mass of the stream’s progenitor, a value that is highly uncertain (see Sect. 4.3) so we cannot use this argument alone to reach any conclusion. The question arise of whether there is any other evidence that supports the hypothesis that the stream have been bound to the SMC-like companion dwarf (DWARF-COMPANION) prior to falling into NGC 7241. The apparently young dynamical age of the stream (see Sect. 6.4 in Leaman et al. 2015) and the similar velocity offset ($\sim 190 \text{ km s}^{-1}$ Leaman et al. 2015) of the stream and

DWARF-COMPANION with respect to the NGC 7241 would seem to favor this scenario. Additionally, if the dwarf irregular satellite is undergoing a relatively recent infall toward NGC 7241 (see further discussion in Sect. 4.5), and thus is still keeping its own substructure (the stream), this may explain why it and the central galaxy seem to show signatures of a recent star formation burst. Whether or not it is expected that an SMC-mass system like the DWARF-COMPANION has a companion dwarf of the mass of the stream progenitor is discussed further in Sect. 4.5. In conclusion, with the current data, we cannot confirm that the stream is associated with the dwarf companion, although none of the analyses presented here disfavor this hypothesis.

4.5. Origin of blue streams: Insights into the Local Group dwarf’s star formation history

Star formation is rarely detected in stellar streams as it requires the presence of dense molecular clouds that would be quickly heated up and destroyed by the many processes involved in the satellite-central galaxy interaction (e.g., Emerick et al. 2016; Cortese et al. 2021). As a consequence, most tidal streams in the local Universe host old stars that were stripped out from the progenitor’s dwarf galaxy by a minor merger event. However, this scenario does not apply to all dwarf-central galaxy interactions. From the theory of galaxy formation and evolution we expect that changes in the mass of the central galaxy modify the efficiency that the gas ram-pressure stripping process has on removing gas from the incoming satellites (Koutsouridou & Cattaneo 2019). These changes probably occurred in the Milky Way and Andromeda galactic systems when transiting from a low-mass system with no warm-hot corona to the current situation with a well defined warm-hot CGM.

In the early scenario where dwarf galaxies merged with a low-mass MW with no well-developed warm-hot CGM, the infalling satellites were able to keep their gas for a long time, and thus we expect they could undergo a strong star formation burst (Di Cintio et al. 2021) similar to the one observed in NGC 7241’s companion or in observations of similar interacting systems (e.g., Kapferer et al. 2009; Beaton et al. 2014). This star formation peak would be clearly reflected in their SFH. Many authors obtained the SFH of the Local Group dwarfs by fitting the color–magnitude diagrams to evolutionary models and reported an SFH with a single peak (Aparicio & Hidalgo 2009; Weisz et al. 2014), and obtained results that may be consistent with the above-mentioned hypothesis and with what is currently occurring in the NGC 7241 system. However the exact shape of the SFH of these objects is difficult to estimate as it depends on multiple variables, for example, more massive and concentrated satellites are more efficient in shielding gas in their central regions from the ram-pressure stripping, so they can keep forming stars for longer times (Cortese et al. 2021; Font et al. 2022). Although this degeneracy is present, a gas-rich dwarf galaxy will always undergo a strong star formation burst in its first interaction with the central galaxy due to compression of molecular clouds induced by tidal forces (Di Cintio et al. 2021). In this scenario it is expected that the gas clouds and stars in the star-forming complexes generated as a consequence of the interaction will be affected by the tidal forces from the central system and will become part of the resulting tidal streams. Therefore, this new stream, at least in the first orbit, will include young stars and gas that has not been yet completely stripped out from the progenitor (i.e., it will show up as a blue stream).

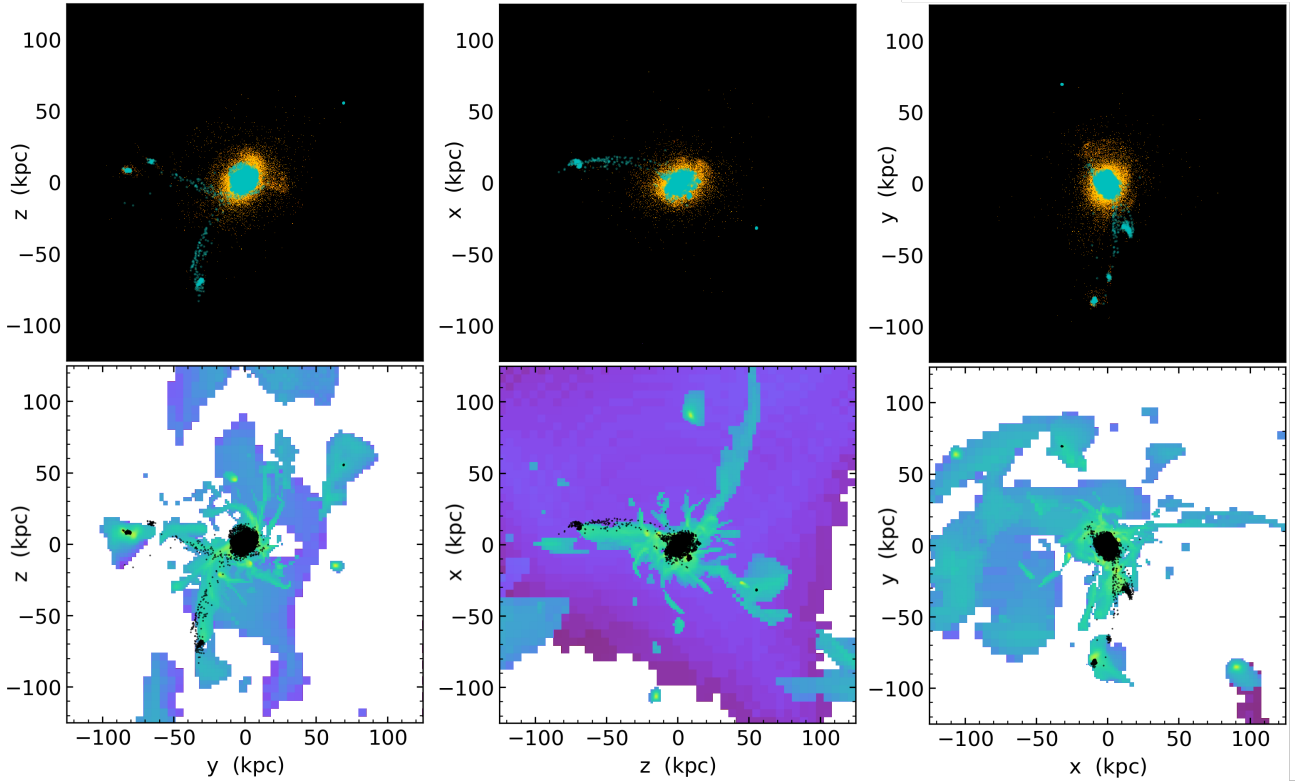


Fig. 5. Blue streams in the GARROTXA cosmological simulation of a $z = 0$ MW-mass galaxy, observed at $z = 1.5$. *Top panels:* total stellar surface luminosity. *Bottom panels:* projected cold gas density ($T < 5 \times 10^4$ K); green-yellow are the high-density gas regions; blue-black are the low-density regions. The cyan dots (left) and black dots (right) show the position of the star particles younger than 350 Myr.

Recent zoomed-in cosmological simulations captured this process at high- z for $z = 0$ MW-mass systems (i.e., when their mass was low enough), showing the formation of blue streams (Roca-Fàbrega et al. 2016; Buck et al. 2019)⁵. An example is the GARROTXA model (Roca-Fàbrega et al. 2016), a high-resolution simulation of the formation of an MW-mass galactic system. In this model we detected that at $z \sim 1.0$ – 1.5 , that is when the progenitor has a mass of $\sim 10^{11} M_{\odot}$, satellites almost reach the galactic disk region without losing their cold gas (see Fig. 5, bottom panels). We observed ongoing strong star formation inside the satellite’s core and also on the stripped stellar stream (i.e., we observed the formation of a blue stream; see Fig. 5, top panels). Interestingly, the satellites contain almost no stars before to their interaction with the MW-mass progenitor; therefore, this interaction induces the first strong star formation episode within them. In this same model we also observed that at $z = 0$ (i.e., when the MW-mass system has already developed a warm-hot gas corona; Roca-Fàbrega et al. 2016), satellites with a similar initial mass and gas content cannot retain their cold gas and show no star formation in the tidal streams.

⁵ In the context of cosmological simulations it is important to mention that this scenario is only weakly dependent on redshift at $z < 1.5$, and that results at $z \sim 1$ can be easily extrapolated to $z = 0$. This is because the minor merger rate is only slowly decreasing at this z (Lotz et al. 2011) and because, although the UV background radiation decays quickly with z (Faucher-Giguère 2020), this has no strong impact on the dense star-forming regions, which are partially or completely self-shielded. Additionally, this weak dependence on z is clearly exceeded by the central galaxy’s mass dependence, as shown above. Thus, we expect that blue streams around low-mass central galaxies exist from high- z ($z \sim 1.5$) down to the local Universe, as confirmed by cosmological simulations.

These results suggest that in the observed blue stream we may be watching a tidally induced star formation burst equivalent to the one that shaped the SFH of some of the dwarf galactic systems in the Local Group (Weisz et al. 2015; Di Cintio et al. 2021) when the MW and Andromeda were low-mass galaxies.

Before finishing the discussion section we want to emphasize that we cannot discard the possibility the blue stream is associated with the star-forming dwarf galaxy (DWARF-COMPANION), not with the NGC 7241 itself. In recent years there has been growing interest in detecting the presence of streams around low-mass galactic systems, LMC- and SMC-like galaxies (e.g., Martínez-Delgado et al. 2012; Kado-Fong et al. 2020). The Λ CDM theory of a hierarchical Universe predicts the presence of very low-mass halos interacting with dwarf galaxies in low-density environments (e.g., Guo et al. 2011; Sales et al. 2013). Some examples of these interactions were recently discovered by the MADCASH Survey (Carlin et al. 2016, 2019). In this context, we propose an alternative scenario: a small galactic system interacted with the DWARF-COMPANION, inducing the observed star formation burst and generating the observed blue stream. Later, both of them fell simultaneously toward the NGC 7241. Metallicity estimations for each of the components in the system could help to reveal which is the true scenario. However, the oxygen abundances we obtained here are too uncertain to allow us to confirm or discard any hypothesis. So, we conclude that more observations are needed to know the real scenario posed by this complex galactic system.

5. Conclusions

In this paper, we characterized the structure of the blue star-forming stream of NGC 7241 discovered by Leaman et al. (2015),

and the kinematics of its most plausible progenitor (STREAM-CORE) using new available images in different broad bands from four independent sources. In order to explore whether this stream had a globular cluster-like progenitor, we obtained follow-up observations using the MEGARA instrument at the GTC in its IFU configuration.

We conclude that the bright compact object (GC-CAND) embedded in the stream, which we initially considered to be the most probable progenitor, is actually a foreground halo star overlapping the path of the stream. However, we report the discovery of a fainter blob in the stream displaying emission lines (STREAM-CORE) that could be interpreted as the actual progenitor displaying a burst of star formation. Our photometric study suggests that this ongoing star formation region detected within the stream produces a near-UV luminosity comparable with that observed in star-forming dwarfs and in the outermost regions of spiral disks. We also measured the width of the stream and obtained values in the range of the observed tidal streams around the Milky Way. Based on these width estimates, we constrained the progenitor's mass, if the stream was created by tidal interaction with NGC 7241, between $6.4 \times 10^6 M_{\odot}$ and $2.7 \times 10^8 M_{\odot}$ when assuming the infall was in a circular orbit. For a more radial orbit, or if it was created by tidal interaction with the (DWARF-COMPANION), this estimate would result in a much lower mass even compatible with that of a massive globular cluster. Although deeper data is needed to distinguish between these possibilities, the NGC 7241 stream is the one with the lowest mass progenitor reported to date, providing a lower limit to the detection of narrow stellar streams beyond the Local Group (see also Pearson et al. 2019, 2022).

Blue star-forming streams like that observed around NGC 7241 should be a common occurrence around galaxies of similar mass. The current galaxy formation and evolution theories predict the presence of these structures around disk galaxies with stellar masses below or around $10^{10.5} M_{\odot}$ that have not developed a warm-hot CGM, and therefore the merging dwarf galaxies can keep their gas for longer times. We show that these structures are also commonly observed in high-resolution cosmological simulations of galactic systems with similar mass as NGC 7241. This scenario also agrees well with the tidal interaction and ram-pressure stripping processes that produced the observed bursty star formation history on some of the Local Group dwarf galaxies followed by a fast quenching (e.g., Kapferer et al. 2009; Di Cintio et al. 2021) when they first entered the virial radius of Andromeda and the MW progenitors (Aparicio & Hidalgo 2009; Weisz et al. 2014).

Acknowledgements. We thanks to Tobias Buck for a fruitful discussion about blue stellar streams in cosmological simulations. We also thanks to the referee for very constructive comments which helped to improve this manuscript. DMD acknowledges financial support from the Talenta Senior Program (through the incentive ASE-136) from Secretaría General de Universidades, Investigación y Tecnología, de la Junta de Andalucía. DMD acknowledges funding from the State Agency for Research of the Spanish MCIU through the “Center of Excellence Severo Ochoa” award to the Instituto de Astrofísica de Andalucía (SEV-2017-0709) and project (PID2020-114581GB-C21/ AEI / 10.13039/501100011033). SRF acknowledges financial support from the Spanish Ministry of Economy and Competitiveness (MINECO) under grant number AYA2016-75808-R, AYA2017-90589-REDT and S2018/NMT-429, and from the CAM-UCM under grant number PR65/19-22462. SRF acknowledges support from a Spanish postdoctoral fellowship, under grant number 2017-T2/TIC-5592. MAGF acknowledges financial support from the MICINN project PID2020-114581GB-C22 grant (Spain). MA acknowledges the financial support from the European Union – NextGenerationEU and the Spanish Ministry of Science and Innovation through the Recovery and Resilience Facility project J-CAVA. JG thanks support from the project AYA2018-RTI-096188-b-i00. JIP acknowledges financial support from projects Estallidos6 AYA2016-79724-C4 (Spanish Ministerio de Economía y Competitividad), Estallidos7 PID2019-107408GB-C44

(Spanish Ministerio de Ciencia e Innovación) and grant P18-FR-2664 (Junta de Andalucía). Based on observations made with the Gran Telescopio Canarias (GTC), installed at the Spanish Observatorio del Roque de los Muchachos of the Instituto de Astrofísica de Canarias, in the island of La Palma. MEGARA has been built by a Consortium led by the Universidad Complutense de Madrid (Spain) and that also includes the Instituto de Astrofísica, Óptica y Electrónica (Mexico), Instituto de Astrofísica de Andalucía (CSIC, Spain) and the Universidad Politécnica de Madrid (Spain). MEGARA is funded by the Consortium institutions, GRANTECAN S.A. and European Regional Development Funds (ERDF), through Programa Operativo Canarias FEDER 2014–2020. This publication is based on observations made on the island of La Palma with the Italian Telescopio Nazionale Galileo, which is operated by the Fundación Galileo Galilei-INAf (Istituto Nazionale di Astrofisica) and is located in the Spanish Observatorio de los Roque de los Muchachos of the Instituto de Astrofísica de Canarias. This project used public archival data from the DESI Legacy Imaging Surveys (DESI LIS). The Legacy Surveys consist of three individual and complementary projects: the Dark Energy Camera Legacy Survey (DECaLS; Proposal ID 2014B-0404; PIs: David Schlegel and Arjun Dey), the Beijing-Arizona Sky Survey (BASS; NOAO Prop. ID 2015A-0801; PIs: Zhou Xu and Xiaohui Fan), and the Mayall z-band Legacy Survey (MzLS; Prop. ID 2016A-0453; PI: Arjun Dey). DECaLS, BASS and MzLS together include data obtained, respectively, at the Blanco telescope, Cerro Tololo Inter-American Observatory, NSF's NOIRLab; the Bok telescope, Steward Observatory, University of Arizona; and the Mayall telescope, Kitt Peak National Observatory, NOIRLab. The Legacy Surveys project is honored to be permitted to conduct astronomical research on Iolkam Du'ag (Kitt Peak), a mountain with particular significance to the Tohono O'odham Nation. NOIRLab is operated by the Association of Universities for Research in Astronomy (AURA) under a cooperative agreement with the National Science Foundation. This project used data obtained with the Dark Energy Camera (DECam), which was constructed by the Dark Energy Survey (DES) collaboration. Funding for the DES Projects has been provided by the U.S. Department of Energy, the U.S. National Science Foundation, the Ministry of Science and Education of Spain, the Science and Technology Facilities Council of the United Kingdom, the Higher Education Funding Council for England, the National Center for Supercomputing Applications at the University of Illinois at Urbana-Champaign, the Kavli Institute of Cosmological Physics at the University of Chicago, Center for Cosmology and Astro-Particle Physics at the Ohio State University, the Mitchell Institute for Fundamental Physics and Astronomy at Texas A&M University, Financiadora de Estudos e Projetos, Fundação Carlos Chagas Filho de Amparo, Financiadora de Estudos e Projetos, Fundação Carlos Chagas Filho de Amparo a Pesquisa do Estado do Rio de Janeiro, Conselho Nacional de Desenvolvimento Científico e Tecnológico and the Ministerio da Ciencia, Tecnologia e Inovacao, the Deutsche Forschungsgemeinschaft and the Collaborating Institutions in the Dark Energy Survey. The Collaborating Institutions are Argonne National Laboratory, the University of California at Santa Cruz, the University of Cambridge, Centro de Investigaciones Energéticas, Medioambientales y Tecnológicas-Madrid, the University of Chicago, University College London, the DES-Brazil Consortium, the University of Edinburgh, the Eidgenössische Technische Hochschule (ETH) Zurich, Fermi National Accelerator Laboratory, the University of Illinois at Urbana-Champaign, the Institut de Ciències de l'Espai (IEEC/CSIC), the Institut de Física d'Altes Energies, Lawrence Berkeley National Laboratory, the Ludwig Maximilians Universität München and the associated Excellence Cluster Universe, the University of Michigan, NSF's NOIRLab, the University of Nottingham, the Ohio State University, the University of Pennsylvania, the University of Portsmouth, SLAC National Accelerator Laboratory, Stanford University, the University of Sussex, and Texas A&M University. The Legacy Surveys imaging of the DESI footprint is supported by the Director, Office of Science, Office of High Energy Physics of the U.S. Department of Energy under Contract No. DE-AC02-05CH1123, by the National Energy Research Scientific Computing Center, a DOE Office of Science User Facility under the same contract; and by the U.S. National Science Foundation, Division of Astronomical Sciences under Contract No. AST-0950945 to NOAO. Based in part on observations at Cerro Tololo Inter-American Observatory, National Optical Astronomy Observatory, which is operated by the Association of Universities for Research in Astronomy (AURA) under a cooperative agreement with the National Science Foundation. Support for this work was provided by NASA through the NASA Hubble Fellowship grant #HST-HF2-51466.001-A awarded by the Space Telescope Science Institute, which is operated by the Association of Universities for Research in Astronomy, Incorporated, under NASA contract NAS5-26555.

References

- Abbott, T. M. C., Abdalla, F. B., Allam, S., et al. 2018, *ApJS*, 239, 18
 Ahumada, R., Prieto, C. A., Almeida, A., et al. 2020, *ApJS*, 249, 3
 Akhlaghi, M. 2019, in *Astronomical Data Analysis Software and Systems XXVI*, eds. M. Molinaro, K. Shorridge, & F. Pasian, *ASP Conf. Ser.*, 521, 299

- Akhlaghi, M., & Ichikawa, T. 2015, *ApJS*, **220**, 1
- Aparicio, A., & Hidalgo, S. L. 2009, *AJ*, **138**, 558
- Barnes, J. E., & Hibbard, J. E. 2009, *AJ*, **137**, 3071
- Beaton, R. L., Martínez-Delgado, D., Majewski, S. R., et al. 2014, *ApJ*, **790**, 117
- Bergemann, M., Hoppe, R., Semenova, E., et al. 2021, *MNRAS*, **508**, 2236
- Bernard, E. J., Ferguson, A. M. N., Schlafly, E. F., et al. 2016, *MNRAS*, **463**, 1759
- Birnboim, Y., & Dekel, A. 2003, *MNRAS*, **345**, 349
- Bonaca, A., Geha, M., Küpper, A. H. W., et al. 2014, *ApJ*, **795**, 94
- Bonaca, A., Conroy, C., Price-Whelan, A. M., & Hogg, D. W. 2019, *ApJ*, **881**, L37
- Bonaca, A., Pearson, S., Price-Whelan, A. M., et al. 2020, *ApJ*, **889**, 70
- Bouquin, A. Y. K., Gil de Paz, A., Muñoz-Mateos, J. C., et al. 2018, *ApJS*, **234**, 18
- Buck, T., Macciò, A. V., Dutton, A. A., Obreja, A., & Frings, J. 2019, *MNRAS*, **483**, 1314
- Bureau, M., Aronica, G., Athanassoula, E., et al. 2006, *MNRAS*, **370**, 753
- Buta, R. J., Verdes-Montenegro, L., Damas-Segovia, A., et al. 2019, *MNRAS*, **488**, 2175
- Carlin, J. L., Sand, D. J., Price, P., et al. 2016, *ApJ*, **828**, L5
- Carlin, J. L., Garling, C. T., Peter, A. H. G., et al. 2019, *ApJ*, **886**, 109
- Castillo-Morales, A. S. P., & Gil de Paz, A. 2020, *MEGARA Data Reduction Cookbook*
- Chilingarian, I., Prugniel, P., Sil'chenko, O., & Koleva, M. 2007, in *Stellar Populations as Building Blocks of Galaxies*, eds. A. Vazdekis, & R. Peletier, *Proc. IAU*, **241**, 175
- Cortese, L., Catinella, B., & Smith, R. 2021, *PASA*, **38**, e035
- Dark Energy Survey Collaboration (Abbott, T., et al.) 2016, *MNRAS*, **460**, 1270
- Dey, A., Schlegel, D. J., Lang, D., et al. 2019, *AJ*, **157**, 168
- Di Cintio, A., Mostoghiu, R., Knebe, A., & Navarro, J. F. 2021, *MNRAS*, **506**, 531
- Duc, P. A., & Mirabel, I. F. 1998, *A&A*, **333**, 813
- Duc, P. A., Brinks, E., Springel, V., et al. 2000, *AJ*, **120**, 1238
- Emerick, A., Mac Low, M.-M., Grcevich, J., & Gatto, A. 2016, *ApJ*, **826**, 148
- Erkal, D., Sanders, J. L., & Belokurov, V. 2016, *MNRAS*, **461**, 1590
- Erkal, D., Koposov, S. E., & Belokurov, V. 2017, *MNRAS*, **470**, 60
- Fardal, M. A., Huang, S., & Weinberg, M. D. 2015, *MNRAS*, **452**, 301
- Faucher-Giguère, C.-A. 2020, *MNRAS*, **493**, 1614
- Font, A. S., McCarthy, I. G., Belokurov, V., Brown, S. T., & Stafford, S. G. 2022, *MNRAS*, **511**, 1544
- Fraternali, F. 2017, *Gas Accretion via Condensation and Fountains*, *Astrophysics and Space Science Library*, ed. A. Fox & R. Davé, **430**, 323
- Gaia Collaboration (Brown, A. G. A., et al.) 2021, *A&A*, **649**, A1
- García-Vargas, M. L., Carrasco, E., Mollá, M., et al. 2020, *MNRAS*, **493**, 871
- Gil de Paz, A., Boissier, S., Madore, B. F., et al. 2007, *ApJS*, **173**, 185
- Giovanelli, R., & Haynes, M. P. 1984, *Bull. Am. Astron. Soc.*, **16**, 961
- Graham, J. A. 1998, *ApJ*, **502**, 245
- Guo, Q., White, S., Boylan-Kolchin, M., et al. 2011, *MNRAS*, **413**, 101
- Hendel, D., & Johnston, K. V. 2015, *MNRAS*, **454**, 2472
- Hester, J. A. 2006, *ApJ*, **647**, 910
- Hibbard, J. E., Bianchi, L., Thilker, D. A., et al. 2005, *ApJ*, **619**, L87
- Howk, J. C., Rueff, K. M., Lehner, N., et al. 2018a, *ApJ*, **856**, 166
- Howk, J. C., Rueff, K. M., Lehner, N., et al. 2018b, *ApJ*, **856**, 167
- Ibata, R. A., Lewis, G. F., Irwin, M. J., & Quinn, T. 2002, *MNRAS*, **332**, 915
- Jennings, Z. G., Romanowsky, A. J., Brodie, J. P., et al. 2015, *ApJ*, **812**, L10
- Johnston, K. V., Sackett, P. D., & Bullock, J. S. 2001, *ApJ*, **557**, 137
- Johnston, K. V., Spergel, D. N., & Haydn, C. 2002, *ApJ*, **570**, 656
- Kado-Fong, E., Greene, J. E., Greco, J. P., et al. 2020, *AJ*, **159**, 103
- Kapferer, W., Sluka, C., Schindler, S., Ferrari, C., & Ziegler, B. 2009, *A&A*, **499**, 87
- Kennicutt, R. C., Jr 1998, *ARA&A*, **36**, 189
- Kereš, D., Katz, N., Weinberg, D. H., & Davé, R. 2005, *MNRAS*, **363**, 2
- Koutsouridou, I., & Cattaneo, A. 2019, *MNRAS*, **490**, 5375
- Lang, D., Hogg, D. W., Mierle, K., Blanton, M., & Roweis, S. 2010, *AJ*, **139**, 1782
- Le Borgne, D., Rocca-Volmerange, B., Prugniel, P., et al. 2004, *A&A*, **425**, 881
- Leaman, R., Erroz-Ferrer, S., Cisternas, M., & Knapen, J. H. 2015, *MNRAS*, **450**, 2473
- Leroy, A. K., Walter, F., Brinks, E., et al. 2008, *AJ*, **136**, 2782
- Lim, B., Sung, H., Bessell, M. S., et al. 2018, *MNRAS*, **477**, 1993
- Lotz, J. M., Jonsson, P., Cox, T. J., et al. 2011, *ApJ*, **742**, 103
- Lu, N. Y., Hoffman, G. L., Groff, T., Roos, T., & Lamphier, C. 1993, *ApJS*, **88**, 383
- Martin, D. C., Fanson, J., Schiminovich, D., et al. 2005, *ApJ*, **619**, L1
- Martínez-Delgado, D., Gabany, R. J., Crawford, K., et al. 2010, *AJ*, **140**, 962
- Martínez-Delgado, D., Romanowsky, A. J., Gabany, R. J., et al. 2012, *ApJ*, **748**, L24
- Martínez-Delgado, D., Cooper, A. P., Román, J., et al. 2023, *A&A*, **671**, A141
- McDonald, M., Bayliss, M., Benson, B. A., et al. 2012, *Nature*, **488**, 349
- Morisset, C., Delgado-Inglada, G., Sánchez, S. F., et al. 2016, *A&A*, **594**, A37
- Mould, J. R., Ridgeway, A., Gallagher, I., J. S., et al. 2000, *ApJ*, **536**, 266
- Noreña, D. A., Muñoz-Cuertas, J. C., Quiroga, L. F., & Libeskind, N. 2019, *Rev. Mex. Astron. Astrofis.*, **55**, 273
- O'Dea, C. P., Baum, S. A., Mack, J., Koekemoer, A. M., & Laor, A. 2004, *ApJ*, **612**, 131
- Pascual, S., Cardiel, N., Picazo-Sanchez, P., Castillo-Morales, A., & Gil De Paz, A. 2018, <https://doi.org/10.5281/zenodo.2206856>
- Pearson, S., Küpper, A. H. W., Johnston, K. V., & Price-Whelan, A. M. 2015, *ApJ*, **799**, 28
- Pearson, S., Price-Whelan, A. M., & Johnston, K. V. 2017, *Nat. Astron.*, **1**, 633
- Pearson, S., Starkeburg, T. K., Johnston, K. V., et al. 2019, *ApJ*, **883**, 87
- Pearson, S., Clark, S. E., Demirjian, A. J., et al. 2022, *ApJ*, **926**, 166
- Price-Whelan, A. M., Johnston, K. V., Valluri, M., et al. 2016a, *MNRAS*, **455**, 1079
- Price-Whelan, A. M., Sesar, B., Johnston, K. V., & Rix, H.-W. 2016b, *ApJ*, **824**, 104
- Roca-Fàbrega, S., Valenzuela, O., Colín, P., et al. 2016, *ApJ*, **824**, 94
- Román, J., Trujillo, I., & Montes, M. 2020, *A&A*, **644**, A42
- Sales, L. V., Wang, W., White, S. D. M., & Navarro, J. F. 2013, *MNRAS*, **428**, 573
- Sengupta, C., Dwarakanath, K. S., & Saikia, D. J. 2009, *MNRAS*, **397**, 548
- Smith, B. J., Struck, C., Hancock, M., et al. 2007, *AJ*, **133**, 791
- Smith, B. J., Giroux, M. L., Struck, C., & Hancock, M. 2010, *AJ*, **139**, 1212
- Tüllmann, R., Rosa, M. R., Elwert, T., et al. 2003, *A&A*, **412**, 69
- Voggel, K. T., Seth, A. C., Baumgardt, H., et al. 2019, *ApJ*, **871**, 159
- Voggel, K. T., Seth, A. C., Sand, D. J., et al. 2020, *ApJ*, **899**, 140
- Wang, H.-F., Hammer, F., Yang, Y.-B., & Wang, J.-L. 2022, *ApJ*, **940**, L3
- Weisz, D. R., Dolphin, A. E., Skillman, E. D., et al. 2014, *ApJ*, **789**, 147
- Weisz, D. R., Dolphin, A. E., Skillman, E. D., et al. 2015, *ApJ*, **804**, 136
- Werk, J. K., Putman, M. E., Meurer, G. R., et al. 2008, *ApJ*, **678**, 888
- Yavetz, T. D., Johnston, K. V., Pearson, S., Price-Whelan, A. M., & Weinberg, M. D. 2021, *MNRAS*, **501**, 1791
- Zou, H., Zhou, X., Fan, X., et al. 2019, *ApJS*, **245**, 4